PNAS

Main Manuscript for

Flying, nectar-loaded honey bees conserve water and improve heat tolerance by reducing wingbeat frequency and metabolic heat production

Authors: Jordan R. Glass[1,2]*, Nicholas P. Burnett[3], Stacey A. Combes[3], Ethan Weisman[1], Alina Helbling[1], and Jon F. Harrison[1]

Affiliations: [1]School of Life Sciences, Arizona State University, Tempe, AZ 85281; [2]Department of Zoology & Physiology, University of Wyoming, Laramie, WY 82071; [3]Department of Neurobiology, Physiology and Behavior, University of California, Davis, CA 95616

Corresponding Author: *Jordan R. Glass, Phone: (480) 338-8271, Email: jrglass84@gmail.com

Classification: Biological Sciences - Physiology

Keywords: Flight kinematics, thermoregulation, flight energetics, evaporative water loss, honey bee, *Apis mellifera*

This PDF file includes:

Main Text

Figures 1 to 7

Abstract

Heat waves are becoming increasingly common due to climate change, making it crucial to identify and understand the capacities for insect pollinators, such as honey bees, to avoid overheating. We examined the effects of hot, dry air temperatures on the physiological and behavioral mechanisms that honey bees use to fly when carrying nectar loads, to assess how foraging is limited by overheating or desiccation. We found that flight muscle temperatures increased linearly with load mass at air temperatures of 20 or 30°C, but, remarkably, there was no change with increasing nectar loads at an air temperature of 40°C. Flying, nectar-loaded bees were able to avoid overheating at 40°C by reducing their flight metabolic rates and increasing evaporative cooling. At high body temperatures, bees apparently increase flight efficiency by lowering their wingbeat frequency and increasing stroke amplitude to compensate, reducing the need for evaporative cooling. However, even with reductions in metabolic heat production, desiccation likely limits foraging at temperatures well below bees' critical thermal maxima in hot, dry conditions.

Significance Statement

Despite the need to be able to predict the effects of climatic warming on animals, we lack methods to assess actual thermal limits of flying insects, such as pollinators. We assessed the relative danger of overheating and desiccation for honey bees carrying loads. Due to the capacity of hot bees to reduce metabolic heat production during flight, our data suggest that under dry and poor forage conditions, desiccation may limit activity before overheating, impairing critical pollination services provided by honey bees.

Main Text

Introduction

Insect pollinators are declining at an alarming rate, due in part to climate change (1). Not only is the planet getting warmer, but it is experiencing increased variation in extreme weather events, such as heat waves (2). These increasingly severe and more frequent thermal events

may push insect pollinators, including bees, beyond their thermal limits, likely exacerbating their decline (3). If insect pollinators continue to decline, we will likely see catastrophic impacts on ecosystems and human agriculture that rely heavily on the ecosystem services provided by these organisms (4-6). In this study, we investigate the air temperatures at which the foraging flights of honey bees (*Apis mellifera*) become heat-limited, and we identify the strategies used by honey bees to avoid and mitigate these limitations. Specifically, we examine the interactions of air temperature, metabolic costs, water balance, and wing kinematics while bees are carrying loads of nectar during flight.

Large flying insects can thermoregulate to some extent, yet their body temperatures typically still rise with external air temperature (7-14). Elevated body temperatures can increase insects' vulnerability to extreme heat events, resulting in reduced foraging and flight durations, or even mortality (3). Most insects evade thermal stress by shifting the time of day during which they are active (15-18). However, many eusocial insects, including honey bees, are obligated to remain active regardless of thermal stress, all to ensure the growth and survival of the colony. Some insects can evaporatively cool to stave off thermal stress (14,15,19-22), but this entails the risk of desiccation. Because metabolic heat production also contributes to an individual's body temperature, several insect species can avoid overheating by lowering their wingbeat frequencies and thus reducing metabolic heat production when flying at high air temperatures (11,21-26). This latter behavioral strategy reduces the risk of desiccation, but lowering wingbeat frequency without changing other aspects of wing kinematics will diminish an insect's aerodynamic lift and mechanical power generation (27) and limit their ability to transport loads of nectar and pollen back to the hive.

To carry heavier loads during flight, animals, such as birds, bats, and bees, must increase their aerodynamic force output (28), which generally results in a higher metabolic cost of flight (29-31). Many flying insects generate aerodynamic force by using a combination of mechanisms, including the sweeping motion of the wing (i.e., wing translation) and by creation of

rotational vortices when the wings rotate before reversing direction. Insects that fly with a large stroke amplitude generate the bulk of their force from the wing translation phase (32), while those that fly with a small stroke amplitude primarily generate significant forces during wing rotation (33). Honey bees lie in the middle of this stroke-amplitude range (amplitude = ~90°), relying on both wing translation and rotation to generate sufficient aerodynamic forces when flying in normal air while free of any pollen or nectar load (34,35).

To generate the additional forces needed to fly in low-density air (since aerodynamic forces decline with air density), honey bees increase their stroke amplitude, presumably increasing translational force production (34,35). Honey bees routinely carry pollen and nectar loads representing 20% and 35% of their body mass, respectively, and have been reported to carry foraging loads up to 80% of body mass (36). However, the kinematic changes used by honey bees to increase force production when carrying resources are unknown. The bumble bee, *Bombus impatiens*, increases stroke amplitude and sometimes wingbeat frequency when carrying heavy loads. But the increased force production required to support these loads cannot be explained solely by changes in frequency and amplitude, suggesting that changes in rotational force production at stroke reversal may also be involved. Heavily loaded *B. impatiens* can carry heavier loads more efficiently (i.e., at lower metabolic cost per unit of added load; 31) than lighter loads, partly by minimizing (or even avoiding) increases in wingbeat frequency, as frequency contributes substantially to metabolic costs in flying bumble bees. Plausibly, honey bees may also be able to increase flight efficiency and thus reduce metabolic heat production to generate the required force to carry large nectar loads without overheating when flying at high air temperatures.

Critical thermal maxima (CT_{max}) are the body temperatures that result in loss of motor control, and measurements of CT_{max} are routinely used to identify temperatures that limit insect survival in heat (37). However, ecological function may be compromised at temperatures much lower than CT_{max}. For flying pollinators, such as honey bees, critical foraging behaviors could be

limited in the heat but below CT_{max} by several potential mechanisms, including desiccation that occurs due to excessive water loss or negative effects of high body temperatures on physiological functions such as power generation by the flight muscles. As yet, we lack the quantitative assessments necessary to determine the environmental conditions that will cause the foraging behavior of pollinators to become heat-limited (3). To determine how high air temperatures affect thermoregulation, water balance, and force generation during foraging flight, we measured flight muscle temperatures, flight metabolic rates, and water loss rates of honey bees carrying nectar loads at three different air temperatures (20, 30, and 40°C), and measured wing kinematics with high-speed video at air temperatures of 25 and 40°C. We then used these data and the prior literature to model heat-limits on honey bee flight.

The metabolic thermal performance curve of flying honey bees that are not carrying any nectar ('unloaded' flight) suggests that flight muscle temperatures greater than 40°C will be associated with progressively lower wing beat frequencies and metabolic rates (11,13), potentially enhancing thermoregulation capacities, but affecting aerodynamic force production in unknown ways. We hypothesized that honey bees flying at high air temperatures generate the forces needed to continue carrying nectar loads primarily by increasing wing stroke amplitude, while lowering wing beat frequencies to reduce metabolic heat production and minimize the level of evaporative cooling required. We further predicted that despite these kinematic adjustments, desiccation would ultimately limit the ability of honey bees to fly in dry air at temperatures substantially lower than the CT_{max} for honey bees (49-50°C; 38,39).

Results

Respirometry Experiments

Flight Muscle Temperature and Flight Metabolism

Unlike other social bees, honey bee workers vary little in body size. We found no significant relationship between body size (averaged wing area, m^2) and total body mass (mg), suggesting the differences in mass between foragers flown at different temperatures are due to the nectar

load these bees carried (LM: $n = 20$, $F_{1,18} = 0.40$, $p = 0.53$; Fig. S1). The effect of nectar loading on flight muscle temperatures depended on the external air temperature (significant air temperature x total body mass interaction term in LMM: $n = 141$, $df = 2$, $\chi^2 = 6.3$, $p = 0.042$). The slope of flight muscle temperature versus total body mass decreased as air temperature rose (Fig. 1A, Table S1). Flight muscle temperatures increased with increasing total body mass (i.e., with nectar loading, since body mass is independent of body size) at 20 and 30°C air temperature (20°C – LM: $n = 48$, $F_{1,46} = 9.1$, $p < 0.001$; 30°C – $n = 46$, $F_{1,44} = 6.9$, $p < 0.01$), but not at 40°C air temperature (40°C – LM: $n = 47$, $F_{1,45} = 0.5$, $p = 0.5$; Fig. 1A).

We did not find a significant interaction between air temperature and nectar load on flight metabolic rate (LMM: $n = 141$, $df = 2$, $\chi^2 = 2.3$, $p = 0.32$). Metabolic rates of honey bees flown at 20 and 30°C air temperature increased with nectar-load with very similar slopes (Fig. 1B; LM: 20°C: slope = 0.38, lower 95% = 0.16, upper 95% = 0.61; 30°C: slope = 0.36, lower 95% = 0.17, upper 95% = 0.56; Table S1). However, at 40°C air temperature, flight metabolic rate was not significantly affected by nectar load (LM: 40°C: slope = 0.18, lower 95% = -0.01, upper 95% = 0.37; Fig. 1B), and average flight metabolic rate was significantly lower than observed at 20 and 30°C air temperature (LMM: $n = 141$, $df = 2$, $\chi^2 = 80.2$, $p < 0.0001$; Fig. 1B inset). Flight metabolic rate increased by about 30% over the full range of masses (Fig. 1B), and the effect of load explains 22% of the variation in flight metabolic rate for the 20 and 30°C air temperature bees pooled (Table S1).

Evaporative Water Loss

Air temperature and total body mass (nectar loading) had a significant interactive effect on water loss rates (LMM: $n = 141$, $df = 2$, $\chi^2 = 8.5$, $p = 0.01$; Fig. 2A), where water loss rates increased with load for bees flown at 40°C air temperature (LM: $n = 47$, $F_{1,45} = 4.2$, $p = 0.046$), but not at 20 or 30°C air temperature (20°C – LM: $n = 48$, $F_{1,46} = 0.45$, $p = 0.51$; 30°C: $n = 46$, $F_{1,44} = 0.001$, $p = 0.93$ Fig. 2). Bees flying at 40°C air temperature had much higher water loss rates (40°C:

150 0.33±0.02 mg $H_2O \cdot min^{-1}$; mean±95% CL) than those flying at 20 and 30°C air temperature (20°C:
151 0.06±0.002 mg $H_2O \cdot min^{-1}$; 30°C: 0.08±0.004 mg $H_2O \cdot min^{-1}$; Fig. 2)

152 *Heat Flux*

153 When data are pooled across all temperatures, there was a strong increase in evaporative heat
154 loss rates when flight muscle temperatures exceeded 40°C (PLM: n = 141, $F_{3,137}$ = 327.8, p <
155 0.0001; Fig. 3). Metabolic heat production increased as flight muscle temperatures increased to
156 39°C, and then decreased at higher flight muscle temperatures (PLM: n = 141, $F_{2,138}$ = 40.2, p <
157 0.0001; Fig. 3)

158 *Limitations on Flight Duration due to Desiccation*

159 Honey bees flying at high air temperatures are in negative water balance (22), so bees flying in
160 search of resources will progressively desiccate faster as air temperature rises. We calculated the
161 maximum flight duration (*MFD*; minutes) a forager can fly without finding nectar or water, which is
162 the flight time until death by desiccation, as:

163 $$MFD = \frac{\text{critical water loss (mg)}}{EWLR - MWP}$$

164 where evaporative water loss rate (*EWLR*) and metabolic water produced (*MWP*) are in $mg \cdot min^{-1}$.
165 To calculate *EWLR* and *MWP*, we determined the linear relationship between air temperature
166 (T_{air}) and flight muscle temperature (T_{thorax}) by fitting a line to our pooled data across the three air
167 temperatures tested (R^2 = 0.85) as:

168 $$T_{air} = \frac{T_{thorax} - 25.313}{0.4684}$$

169 Next, we fit a polynomial model relating T_{air} to *EWLR* using our pooled data (R^2 = 0.88):

170 $$EWLR = \left(1.84 \cdot 10^{-5} \times {T_{air}}^3\right) - \left(7.73 \cdot 10^{-4} \times {T_{air}}^2\right) + \left(7.52 \cdot 10^{-3} \times T_{air}\right) + 0.06$$

Metabolic water production was calculated assuming that one mole of water is produced per mole of carbon dioxide produced. The polynomial relationship between *MWP* and T_{air} in our pooled data (R^2 = 0.37) was:

$$MWP = \left(-1.46 \cdot 10^{-4} \times {T_{air}}^2\right) + \left(7.76 \cdot 10^{-3} \times T_{air}\right) + 0.014$$

Resting honey bees die at a water content of ~74% (wet mass divided by dry mass; 39), indicating that an unloaded bee (average mass: 70 mg) that cannot find external sources of water to aid in evaporative cooling may lose at most 18 mg of internal water before death, so we used this as our estimate of critical water loss.

These calculations suggest that hot, dry air temperatures may limit honey bee foraging due to desiccation. Between 20 and 32°C air temperature, metabolic water production rates exceed evaporative water loss, suggesting bees can fly without desiccating (Fig. 4). However, in dry air, desiccation-limited flight durations strongly decline as air temperatures exceed 33°C (Fig. 4). In 40°C dry air, a 70 mg honey bee loses water at about 0.3 mg·min^{-1} (Fig. 4), but produces metabolic water at only about 0.09 mg·min^{-1}. At 40°C air temperature, a flying bee will desiccate to its critical water content after about 1.5 hours (Fig. 4). At 46°C, bees will desiccate to death in just over 30 minutes (Fig. 4), near the duration of an average foraging trip for a honey bee (36).

Kinematics Experiment

Wingbeat Frequency

Honey bees flying at 40°C air temperature displayed lower average wingbeat frequencies (211.0±4.7 Hz; mean±95% CL) than at 25°C air temperature (234.7±4.2 Hz; GLM: n = 89, df = 1, χ^2 = 8.2, p = 0.004; Fig. 5). There was also a significant effect of nectar load (GLM: n = 89, df = 1, χ^2 = 13.2, p < 0.001), and a significant interactive effect between air temperature and nectar load (GLM: n = 89, df = 1, χ^2 = 3.9, p = 0.048) on wingbeat frequency. When analyzed separately, bees flown at 40°C significantly increased their wingbeat frequency when carrying heavier nectar

loads, but bees flown at 25°C did not (25°C – linear regression: $F_{1,41} = 1.7$, $p = 0.2$; 40°C – linear regression: $n = 46$, $F_{1,44} = 13.8$, $p < 0.001$).

Stroke Amplitude

Nectar-carrying foragers displayed higher average stroke amplitudes at 40°C air temperature (98.7±3.1°) than at 25°C (90.0±4.1°; GLM: $n = 89$, $df = 1$, $\chi^2 = 17.3$, $p < 0.001$; Fig. 6 inset). Bees flying at both 25 and 40°C air temperature increased stroke amplitude with increasing total body mass (GLM: $n = 89$, $df = 1$, $\chi^2 = 10.4$, $p < 0.01$; Fig. 6).

Translational Force and Translational Power Proxy

Nectar foragers flying at both 25 and 40°C air temperature increased their translational force production by 42% across the range of total body masses (GLM: $n = 89$, $df = 1$, $\chi^2 = 23.9$, $p < 0.001$; Fig. 7). Similarly, bees flying at both air temperatures strongly increased their translational power proxy with increasing nectar load (GLM: $n = 89$, $df = 1$, $\chi^2 = 24.3$, $p < 0.001$; Fig S2) and their average wingtip velocity (GLM: $n = 89$, $df = 1$, $\chi^2 = 24.1$, $p < 0.001$; Fig. S3). However, translational force, our power proxy, and wingtip velocity were not significantly affected by air temperature (force: GLM: $n = 89$, $df = 1$, $\chi^2 = 0.1$, $p = 0.7$; power proxy: GLM: $n = 89$, $df = 1$, $\chi^2 = 0.003$, $p = 0.96$; wingtip velocity: GLM: $n = 89$, $df = 1$, $\chi^2 = 0.12$, $p = 0.73$).

Discussion

Our results show that honey bees flying at high temperatures can modulate their wing kinematics to reduce flight metabolic rate, lowering their risk of overheating. Bees flying at 40°C air temperature displayed lower average wingbeat frequencies, lower flight metabolic rates, and lower metabolic heat production than bees flying at 25°C (Figs. 1, 3, 5). These findings confirm previous observations of reduced flight metabolic rate in honey bees at high flight muscle temperatures, associated with a decrease in wingbeat frequency (11,22; Fig. 5). At the same time, bees flying at 40°C air temperature displayed higher average stroke amplitudes than those flying at 25°C (Fig. 6), such that translational force generation (Fig. 7), power (Fig. S2), and

wingtip velocity (Fig. S3) were determined by load but not affected by the body temperature of the bee. Bees were thus able to support the same total mass (body mass plus nectar load) when flying at different temperatures by adjusting the relative contributions of two basic kinematic features – wingbeat frequency and stroke amplitude.

The mechanisms by which flight kinematics influence metabolic heat production remain somewhat unclear. Previous work on bumble bees suggests that flight metabolic rate is strongly tied to wingbeat frequency, but is less dependent on stroke amplitude (31). One possible explanation for this pattern might be that changes in frequency and amplitude differentially alter the relative contribution of induced, profile, and inertial power to total mechanical power output. Mathematical predictions suggest that inertial power requirements are more strongly increased by higher wingbeat frequencies than induced or profile power requirements (40,41). Thus, unloaded, cool honey bees may increase heat production when their thorax temperatures are below optimal by elevating wingbeat frequencies and the proportion of total power devoted to overcoming wing inertia, increasing heat production relative to bees flying in warm air. As bees are loaded at air temperatures of 30°C or lower, they maintain these high wingbeat frequencies and produce increased power (and metabolic rate) primarily by increasing stroke amplitude. Unloaded bees flying at 40°C air temperature lower their wingbeat frequencies but increase stroke amplitudes, maintaining similar translational force production, with the lower metabolic heat production potentially due to a lower proportion of total power being used to overcome wing inertia. However, the most heavily loaded bees flying in 40°C air had lower metabolic rates than bees flying in 20 or 30°C air despite having similar wing beat frequencies, stroke amplitudes, and translational power production, suggesting that additional mechanisms for increasing efficiency of hot flight muscles are likely. Metabolic rates of bees flying in 40°C air could potentially be decreased by a combination of factors that may include increased elastic energy storage, changes in wing motions that affect the lift coefficient and/or rotational forces, or decreases in the frequency and magnitude of translational body movements.

In addition to lowering their wingbeat frequency to reduce metabolic heat production, bees flying at 40°C air temperature dramatically increased their rates of evaporative water loss (Fig. 2). These two mechanisms contributed approximately equally to preventing overheating in bees flying at 40°C: kinematic changes reduced metabolic heat production by 11.5 mW on average, and increased evaporative water loss caused a heat flux of 10 mW from the body (Fig. 3).

Depression of metabolic rate through kinematic changes (lowering wingbeat frequency and increasing stroke amplitude) is critical for bees to fly for extended periods in the heat. If bees maintained the same metabolic rates at 40°C air temperature as at 30°C, they would need to double their rate of evaporative cooling to keep their flight muscles from rising above 45°C (Fig. 1). An unloaded honey bee (70 mg) flying at 40°C air temperature that did not depress its metabolic rate through kinematic changes would be forced to increase evaporative water loss to 0.6 $mg \cdot min^{-1}$, cutting the bee's maximal flight time to about 45 minutes, well within the range of normal foraging times. At 46°C air temperature, without suppression of flight metabolic rate, flying bees would desiccate to death in less than 15 minutes in dry air, severely hampering foraging.

Remarkably, honey bees in the respirometry trials flying at 40°C air temperature were able to carry loads up to 60% of their body mass without heating up (Fig. 1A). Although we found no significant interaction between the effects of air temperature and nectar load on flight metabolic rate (Fig. 1B), bees flying at 40°C air temperature had lower flight metabolic rates that did not seem to increase with loading (Fig. 1B; 1B inset). This contrasts with bees flying at 20°C or 30°C air temperature, whose flight muscle temperatures and metabolic rates both increased with additional loading (Fig. 1). Bees flying at 25°C displayed high wingbeat frequencies that were independent of total body mass, suggesting that bees use a less efficient kinematic strategy when flying in cool air, perhaps to generate additional metabolic heat and warm themselves toward 39°C, the flight muscle temperature associated with maximal flight metabolic rate (13).

Even though bees with flight muscle temperatures of 45°C could carry nectar loads up to 60% of their body mass in our study, it remains possible that high air and flight muscle temperatures may impose some limits on the load-carrying capacity of honey bees. The force production of tethered bees declines at flight muscle temperatures above 40°C (42), and we did not explicitly design these experiments to test whether load-lifting capacity is reduced as muscle temperatures rise. Flying honey bees can pick up and remove dead bees weighing near their body mass, and bees' ability to carry these types of extreme loads may become limited at higher air temperatures. Nonetheless, our data demonstrate that metabolic rate and heat production can be, to a substantial extent, uncoupled from the production of excess lift, and that bees with flight muscle temperatures of 45°C can carry nectar loads up to 50 mg, well above typically observed nectar loads of 30 mg or less (36).

Several caveats must be considered regarding our conclusions, however. First, CO_2-production rates in the respirometry trials were averaged over 10 seconds of flight, whereas wing kinematics were analyzed over approximately 0.05 seconds. Plausibly, in the time-averaged respirometry measurements, other behaviors may vary with temperature, such as the amount of side-to-side movement, or the distance of bees from the edges of the flight chamber. Moreover, bees in the respirometry trials were flown in a relatively small chamber (i.e., ~350 ml cylindrical chamber) with relatively high air flow rates, creating the possibility of turbulence and edge effects that might alter flight behavior and metabolic cost. A final consideration is that the Arizona and California bees could potentially differ in their thermal biology, though we found similar flight muscle temperatures and wing beat frequency changes with temperature.

Our study challenges the approach of using CT_{max} values of resting ectotherms to estimate the limits posed by high temperatures in the field. At extremely high air temperatures, flight muscle temperatures are predicted to be 1-2°C above air temperature (22). If the CT_{max} of resting bees is 49°C (3), brief periods of flight should be possible at air temperatures approaching 48°C. However, in dry air at temperatures of 45°C or higher, bees will die from desiccation over

normal foraging trip durations if they are unable to find nectar or water, suggesting that desiccation can limit foraging at significantly lower air temperatures than CT_{max}. It is important to note that our estimates of maximal flight times before desiccation may be higher than actual, if the physiological function of bees is impaired at water contents higher than those that cause death. Humidity, wind speed, and solar radiation will have additional, unknown effects on the heat limitations on foraging honey bees and other pollinators. Empirical tests of the interactions between humidity, temperature, solar radiation, and wind speed on flight metabolic rate, thermoregulation, and load-carrying capacities will be required to predict honey bee foraging across the full range of environmental conditions that will be experienced with future climate change. However, our data suggest that desiccation will begin to limit foraging by honey bees at air temperatures of 46°C or higher, unless consistent and substantial nearby sources of nectar are available.

Materials and Methods

Respirometry Measurements

Study Animals and Location

We conducted experiments to measure the effect of air temperature on body temperatures, metabolic rates, and water balance using three colonies of honey bees, *Apis mellifera*, maintained at Arizona State University (ASU) in Tempe, AZ, USA. We captured unloaded (i.e., carrying no nectar), outgoing foragers who were leaving the colony. We recorded each bee's pre-fed (unloaded) mass (average mass: 70 mg), fed it a randomized amount of 50% sucrose solution [ranging from 0 µL (leaving the mass of the bee unchanged) to 45 µL], and then recorded its fed mass. We measured the flight metabolic rates of fed bees inside a temperature-controlled room (Environmental Growth Chamber; Chagrin Falls, Ohio, USA) set to either 20±0.5, 30±0.5, or 40±0.05°C air temperature. We monitored the temperature inside the room using a thermocouple integrated with Expedata (Sable Systems, Las Vegas, NV). We used a random number generator to decide the order in which colonies were sampled.

Metabolic and Water Loss Rate Measurements

Immediately after feeding, we transferred each bee to a respirometry system in the temperature-controlled room to measure metabolic rate during flight. To do this, we placed the bee in a cylindrical, transparent-acrylic flight chamber (350 mL), which was sealed and covered with a dark cloth for approximately two minutes to reduce the bees' activity before the flight trial began. We used a flow meter (Alicat Scientific, Inc., Tucson, AZ) to produce 2 $L \cdot min^{-1}$ air flow, which passed sequentially through a $CaSO_4$ and soda lime column to remove H_2O and CO_2 and then to the reference cell of the LI-COR LI-7000 CO_2/H_2O analyzer (Lincoln, NE, USA). Next, the air flowed to the respirometry chamber where the bee was flying, and then to the sample cell of the LI-7000. The differential analog output from the LI-COR was digitized (Sable Systems UI-2) and recorded each second (Expedata, Sable Systems, Las Vegas, NV). The LI-7000 was CO_2 calibrated using 100.4 ppm CO_2 and Ultra-Zero calibration gases at the same flow rate and pressures as during flight respirometry, and baseline recordings were taken before and after each measurement period. The LI-7000 was also calibrated for H_2O by performing a steady-state volts versus water concentration model, which involved injecting increasing of water (1 to 10 µL into the flow-stream of the analyzer and using the resulting integrated voltage-time output to create a calibration curve; 43).

Before the flight trial began, while the bee sat in darkness, we flushed the chamber for three minutes, allowing CO_2 and H_2O levels flowing from the chamber to the LI-7000 to reach a low, stable level. In each flight trial, we encouraged bees to hover for six minutes by shining a 150W, dual goose-neck Fiber Optical Illuminator (China) over the chamber. Bees that landed were immediately encouraged to fly by gently tapping and inverting the chamber. Bees that did not fly for at least 75% of the flight trial were removed from the study. Here, we define 'flight' as the bee flying freely and maintaining its altitude above the bottom third of the chamber, without touching the sides. We used Expedata to identify and calculate average data from the

ten seconds with the most stable CO_2 and H_2O readings that represented continual free-flight during each trial.

We calculated CO_2 emission rates ($\dot{V}_{CO_2}$; $mL \cdot h^{-1}$) by multiplying the differential CO_2 fraction times the standard temperature and pressure (STP) flow-rate through the flight chamber (43). Then, to calculate the flight metabolism (mW), synonymous with metabolic heat production, we multiplied $\dot{V}_{CO_2}$ by the energy yield per amount of CO_2 formed, 21.146 $J \cdot mL^{-1}$ CO_2, assuming simple carbohydrate catabolism (44-46). We calculated flight water loss rate ($\dot{V}_{H_2O}$, mg $H_2O \cdot h^{-1}$) by multiplying the fractional concentration of water ($mmol \cdot mol^{-1}$) leaving the chamber by the STP flow rate ($ml \cdot min^{-1}$) and the molar mass of water (18 $g \cdot mol^{-1}$), then dividing by the molar volume of water found in one-liter of air at STP (22,400 $ml \cdot mol^{-1}$). We calculated evaporative heat loss (mW) by multiplying $\dot{V}_{H_2O}$ by the latent heat of evaporation of water (2.41 $J \cdot mg$ of $water^{-1}$).

Flight Muscle Temperature Measurements

We measured the flight muscle temperature of each bee immediately after the flight trial by quickly transferring the bee into a plastic bag, flattening the bag to restrict the bee's movement, and then inserting a Physitemp model MT29/1 hypodermic microprobe (Clifton, New Jersey, USA; 29-gauge, time constant=0.025·s) through the bag and into the center of the thorax. We recorded flight muscle temperature data with a Pico Technology USB TC-08 Thermocouple Data Logger (Tyler, TX, USA), measuring flight muscle temperature within three seconds of cessation of flight after the bee had flown for at least one minute to ensure their flight muscles were at a stable thermal equilibrium (22), and recording the highest temperature reported by the thermometer. If measurements took longer than five seconds to measure, we excluded the bee's temperature measurement from the analysis. Finally, we weighed the bee (±0.1 mg) using an A&D HR-120 Analytical Balance (Tokyo, Japan) and stored its body at -20°C.

Statistical analyses

We used linear mixed-effects models (LMM) to test the independent and interactive effects of air temperature (°C) and total body mass (mg) on flight metabolic rate [milliwatts ($mJ \cdot s^{-1}$)], flight muscle temperature and water-loss rate (mg $H_2O \cdot min^{-1}$), with colony included as a random effect. Any reported interactive or independent effects come from full models [e.g., flight metabolic rate ~ air temperature x total body mass + (1|colony)] after running a type III ANOVA on the model output. We used linear regression models (LM) after running the full model if there was a significant interactive effect of the two independent variables in the full models to examine the separate effects of air temperature and total body mass. We ran general linear models (GLM) on the above-mentioned variables if the random effect of 'colony' was negligible, and linear regression models if a reduced model with one independent predictor was a better fit. We used polynomial linear regression models (PLM) to determine the best polynomial fit for measures of metabolic heat production and evaporative heat loss. Best models were chosen using the Akaike Information Criterion (AIC) and the Bayesian Information Criterion (BIC). For the respirometry and kinematic experiments, data were analyzed using R (3.6.2; R Foundation for Statistical Computing, Vienna, Austria), specifically using the 'Matrix', lmer', and 'car' packages, and two-tailed significance was determined at $\alpha = 0.05$.

Kinematic Measurements:

Study Animals and Location

We conducted experiments examining the effect of temperature on wing kinematics during loaded flight on honey bees captured while foraging on flowers, on the campus of the University of California, Davis. Data collection took place from May 29 to June 3, 2022, from approximately 8:00 to 18:00 each day. We captured individual foragers using a 45-ml conical centrifuge tube and weighed them within two minutes using an Ohaus Explorer EX124 balance (±0.1 mg). Our analysis assumes that all the honey bees in our study have a similar unloaded (no nectar) mass (average mass: 70 mg) due to the narrow variation in body size that occurs in *A. mellifera.* The observed mass of each bee was therefore considered to be the bee's unloaded mass plus

399 additional mass due to some volume of nectar, as pollen foragers were excluded from this study.
400 We used the naturally occurring range of nectar loads in the foraging bees to assess the effect of
401 nectar load on flight kinematics and thermoregulation at two different air temperatures (25 and
402 40°C).

403 *Flight Trials*

404 After recording the bee's mass, we moved the bee into our custom, temperature-controlled flight
405 chamber (17.8 cm x 16.5 cm x 25.6 cm; width x height x length). The temperature of the chamber
406 was set between trials by allowing cooled (25±0.25°C) or heated air (40±0.25°C) to flow through
407 the chamber until the desired temperature was achieved. Each bee was flown in the chamber
408 only once and at a single temperature for a six-minute flight duration. The chamber was lit from
409 above and the side using 23-Watt LED light bulbs (2610 Lumens, 3000K bright white; Great
410 Eagle, Boca Raton, FL, USA).

411 We filmed flights with two synchronized, manually triggered high-speed video cameras
412 (Phantom V611, Vision Research, Inc., Wayne, NJ, USA) sampling at 3000 frames·s^{-1} (exposure
413 time: 20 μs), positioned above and in front of the flight chamber. We calibrated cameras with a
414 standard checkerboard calibration method and built-in MATLAB functions (47,48). This method
415 captures lens distortion and projective geometry (using intrinsic parameters), as well as the global
416 positions and orientations of the cameras relative to the flight chamber (via extrinsic parameters).

417 We encouraged each bee to fly in the chamber by using the chamber lighting or by
418 tapping the chamber and by waving a small, plumose feather outside of the chamber. Once the
419 bee exhibited stable, hovering flight, we recorded a high-speed video that was at least 0.1 second
420 long. We used the definition of hovering flight proposed by Ellington (28) to determine whether
421 the body motions of bees during our flight sequences were slow enough that bees are likely to
422 display kinematics and aerodynamics indistinguishable from those seen during force equilibrium
423 (true hovering). Ellington calculated the non-dimensional flight velocity of his sequences (V/nR, or
424 body velocity divided by wingbeat frequency times wing span), which represents the number of

wing lengths traveled per wingbeat. He applied a conservative definition in his study of hovering flight and used only 11 flight sequences in which non-dimensional flight velocity was 0.40 or below. We calculated the non-dimensional flight velocity of all sequences in our study and found that our reported values fall well within the range considered to be hovering flight: average non-dimensional flight velocity was 0.11 and the maximum non-dimensional flight velocity in any sequence was 0.23. After the flight recording, we recorded the bee's final, post-flight mass and transferred it to a -20°C freezer for storage.

Wing Length and Wing Area Measurements

We measured the average forewing length (mm) and wing area of the fore- and hindwings together (mm^2) using an image processing program (ImageJ; https://imagej.net/ij/). We randomly selected ten frozen bees from each temperature group, then removed each bee's right fore- and hindwings, repositioned them to resemble their relative positions during flight, and photographed them. We repositioned the fore- and hindwings as close to their natural, connected position as possible because we found significant differences between wing-area calculations of separated versus overlaid wings. There was no significant difference between the mean wing length [$t_{(18)}$ = 0.4, p = 0.73] or wing area [$t_{(18)}$ = 0.1, p = 0.90] of randomly sampled bees that were flown at either 25 or 40°C air temperature.

Video Analysis

For each video, we tracked four landmarks on the bees: the head, the posterior tip of the abdomen, and the base and tip of one of the wings. We digitized the two-dimensional positions of these landmarks in every frame from each camera view using DLTdv6 (49) in MATLAB, and then converted these into three-dimensional coordinates using the camera calibration and built-in MATLAB functions, following Burnett *et al*., (2020; 50). We filtered three-dimensional position data using a 5th-order, low-pass Butterworth filter with a cut-off frequency of 100 Hz to remove errors due to the digitization process, following Ravi *et al*. (2022; 51). The wing stroke plane of bees is not always perfectly horizontal; thus, to quantify wing position within the stroke plane of

each flight, we shifted positional data into their principal axes (i.e., shifted to a horizontal stroke plane angle) using a principal components analysis. We used the adjusted position data in each frame to calculate a time-series of wing position angle (i.e., sweep) within the stroke plane, via the four-quadrant inverse tangent function in MATLAB. We calculated stroke amplitude (Φ; °) for each flight by using the average amplitude of three half-strokes (i.e., maximum wing angle minus minimum wing angle in each half-stroke). Similarly, we used the time-series of wing angle to calculate wing beat frequency (n; Hz), dividing the number of complete wing beats digitized by the total duration. We calculated the average arc length (a) of the stroke by converting the average stroke amplitude from degrees to radians, then multiplying this by 75% of the wing length, to avoid the portion of the wing that may deform during the stroke (31). We then calculated the average wing velocity, U_w ($m \cdot sec^{-1}$) as $2a$ (to include the total arc length of the up- and downstroke) multiplied by the wingbeat frequency, n.

We estimated the total force produced during wing translation (F_{tr}) for bees carrying various nectar loads while flying at either 25 or 40°C air temperature using the following equation:

$$F_{\mathrm{tr}} = \frac{1}{2}\rho C_L {U_w}^2 \mathrm{S}$$

where ρ is air density ($kg \cdot m^{-3}$), C_L is the estimated lift coefficient (0.74), U_w is the average wing velocity ($m \cdot s^{-1}$), S is the averaged wing area (m^2). We calculated this rough estimate of the forces produced only during the wing translation phase of the stroke cycle, to determine how measured changes in frequency and amplitude (which determine wing velocity, U_w) affected this component of force production. This estimate is only approximate because we do not have an accurate lift coefficient for our bees' wings, or measurements of how wing angle of attack changed during translation. We could not calculate total aerodynamic force produced during the wing stroke, as we did not have the data necessary to calculate the forces generated by wing rotation, or the correction factors needed to estimate the temporal and spatial nature of vortex shedding (40,41).

475 However, to determine whether the relative contributions of translational and rotational
476 forces to total force production differed substantially between bees flying at 25 and 40°C air
477 temperature, we compared the slopes of translational force vs. total body mass for bees flying at
478 these air temperatures (Fig. 7). We also estimated the proportion of total flight force contributed
479 by the translational portion of the wing-stroke, by dividing the translational force (F_{tr}) by the total
480 force (F) required to support a bee's total weight while hovering:

481 $$F = (m \cdot g)$$

482 where m is the mass of the animal (in grams) and g is the gravitational acceleration (9.81 $m \cdot s^{-2}$).

483 We also estimated the power exerted by the wings on the surrounding air during the
484 translational phase of the wing stroke (translational power, P_{tr}):

485 $$P_{\mathrm{tr}} = \rho S {U_w}^3$$

486 where ρ is air density ($kg \cdot m^{-3}$), S is the averaged wing area (m^2), and U_w is the average wing
487 velocity ($m \cdot s^{-1}$). Our conservative approach reports only the measured component of
488 aerodynamic power rather than reporting an estimate of total mechanical power output based on
489 numerous assumptions (as in 31).

490 *Statistical analysis*

491 We used a GLM to test the independent and interactive effects of air temperature and
492 total body mass (i.e., unloaded body mass plus nectar load) on wingbeat frequency, stroke
493 amplitude, translational force, and translational power proxy. Flight trials were excluded if bees
494 did not fly successfully in the chamber for at least 75% of the flight trial or if the bees flew outside
495 of the field of view of the high-speed cameras. We analyzed each type of model with a type III
496 ANOVA. Models were chosen using the Akaike Information Criterion (AIC) and the Bayesian
497 Information Criterion (BIC) where each model comparison consisted of dropping a single
498 explanatory variable. If there were no significant interactions between explanatory variables, a

type II ANOVA was used on the model outputs to increase explanatory power. If there was a significant interaction between air temperature and total body mass, we used linear regression analyses (LM) to test whether the slope of the fitted lines for each temperature were significantly different from zero.

Acknowledgments

We would like to thank Arron Montelongo and Andrea Brandt for experimental assistance. Special thanks to Christine Glass and Stav Talal for their constructive conversations. We would like to thank Robert Dudley, Dale DeNardo, and Jennifer Fewell for feedback on this manuscript, as well as the Harrison lab for beneficial comments. Additional thanks to Jason Vance for his helpful advice, feedback, and encouragement. Thanks goes to Dan Campbell, Casey Cavaliere, Matt Brasch, Josh Martin, Nick Steinborn, and Mike Kennedy for motivation. We would also like to thank Arizona State University and the University of California, Davis for allowing us to use their facilities, and Cahit Ozturk for hive maintenance of colonies used for this experiment. Portions of this paper were developed from the thesis of J. R. G. This study was funded by the Research and Teaching Initiative at Arizona State University (J.R.G) and the United States Department of Agriculture (grant no. 2017-68004-26322) (J.F.H.).

Author Contributions: J.R.G.: conceptualization, data curation, formal analysis, investigation, methodology, validation, visualization, writing— original draft, writing—review and editing; N.P.B.: methodology, formal analysis, writing—review and editing; S.A.C: methodology, writing—review and editing; E.W.: investigation, formal analysis, writing—review and editing; A.H.: investigation, writing—review and editing; J.F.H.: conceptualization, funding acquisition, project administration, resources, supervision, writing—review and editing.

Competing Interest Statement: Authors declare they have no competing interests.

References

1. Halsch, C.A., Shapiro, A.M., Fordyce, J.A., Nice, C.C., Thorne, J.H., Waetjen, D.P., and Forister, M.L. (2021). Insects and recent climate change. *Proceedings of the National Academy of Sciences*, *118*(2), e2002543117.

2. IPCC. Summary for Policymakers (2021). Allan, R.P., Arias, P.A., Berger, S., Canadell, J.G., Casou, C., Chen, D.L., Cherchi, A., Connors, S.L., Coppola, E., Cruz, F.A., *et al*., Summary for Policymakers. Climate Change 2021: The Physical Science Basic: Working Group I Contribution to the Sixth Assessment Report of the Intergovernmental Panel on Climate Change. Cambridge University Press.
3. Johnson, M.G., Glass, J.R., Dillon, M.E., and Harrison, J.F. (2023). How will climatic warming affect insect pollinators?. In *Advances in Insect Physiology*, *Academic Press Inc., 64, 1-115*.
4. Lever, J. J., van Nes, E. H., Scheffer, M., and Bascompte, J. (2014). The sudden collapse of pollinator communities. *Ecology Letters*, *17*(3), 350–359.
5. van der Sluijs, J.P. (2020). Insect decline, an emerging global environmental risk. *Reflections on Advances in Health and Environment Research in the Context of the COVID-19 Pandemic*, *46*, 39–42.
6. Ramos-Jiliberto, R., Moisset de Espanés, P., and Vázquez, D.P. (2020). Pollinator declines and the stability of plant–pollinator networks. *Ecosphere*, 11, e03069.
7. Heinrich, B. (1971). Temperature regulation of the Sphinx Moth, *Manduca sexta*: I. Flight energetics and body temperature during free and tethered flight. *Journal of Experimental Biology*, *54*(1), 141-152.
8. Heinrich, B. (1972a). Temperature regulation in the bumblebee *Bombus vagans*: a field study. *Science*, *175*(4018), 185-187.
9. Heinrich, B. (1972b). Energetics of temperature regulation and foraging in a bumblebee, *Bombus terricola* Kirby. *Journal of Comparative Physiology*, *77*(1), 49-64.
10. Heinrich, B. (1980a). Mechanisms of body-temperature regulation in honeybees, *Apis mellifera* I. Regulation of head temperature. *Journal of Experimental Biology*, *85*(1), 61-72.
11. Harrison, J.F., Fewell, J.H., Roberts, S.P., and Hall, H.G. (1996). Achievement of thermal stability by varying metabolic heat production in flying honeybees. *Science*, *274*(5284), 88-90.
12. Woods Jr, W. A., Heinrich, B., & Stevenson, R. D. (2005). Honeybee flight metabolic rate: does it depend upon air temperature? *Journal of Experimental Biology*, *208*(6), 1161-1173.
13. Glass, J.R. and Harrison, J.F. (2022). The thermal performance curve for aerobic metabolism of a flying endotherm. *Proceedings of the Royal Society B*, *289*(1981), 20220298.
14. Johnson, M.G., Glass, J.R., and Harrison, J.F. (2022). A desert bee thermoregulates with an abdominal convector during flight. *Journal of Experimental Biology*, *225*(19), jeb244147.
15. Cooper, P.D., Schaffer, W.M., and Buchmann, S.L. (1985). Temperature regulation of honey bees (*Apis mellifera*) foraging in the Sonoran Desert. *Journal of Experimental Biology*, *114*(1), 1-15.
16. Bergman, P., Molau, U., and Holmgren, B. (1996). Micrometeorological impacts on insect activity and plant reproductive success in an alpine environment, Swedish Lapland. *Arctic and Alpine Research*, *28*(2), 196–202.
17. Pyke, G.H., Inouye, D.W., and Thomson, J.D. (2011). Activity and abundance of bumble bees near Crested Butte, Colorado: Diel, seasonal, and elevation effects. *Ecological Entomology*, *36*(4), 511–521.
18. Di Trani, J.C., Ramírez, V.M., Añino, Y., and Barba, A. (2022). Environmental conditions and bee foraging on watermelon crops in Panama. *Journal of Animal Behaviour and Biometeorology*, *10*(4), 2234–2234.
19. Heinrich, B. (1980b). Mechanisms of body-temperature regulation in honeybees, *Apis mellifera* II. Regulation of thoracic temperature at high air temperatures. *Journal of Experimental Biology*, *85*(1), 73-87.

20. Nicolson, S.W. and Louw, G.N. (1982). Simultaneous measurement of evaporative water loss, oxygen consumption, and thoracic temperature during flight in a carpenter bee. *Journal of Experimental Zoology*, *222*(3), 287-296.
21. Cooper, P.D., Schaffer, W.M., and Buchmann, S. L. (1985). Temperature regulation of honey bees (Apis mellifera) foraging in the Sonoran desert. *Journal of Experimental Biology*, *114*(1), 1-15.
22. Roberts, S.P. and Harrison, J.F. (1999). Mechanisms of thermal stability during flight in the honeybee *Apis mellifera*. *Journal of Experimental Biology*, *202*(11), 1523-1533.
23. Chappell, M.A. (1984). Temperature regulation and energetics of the solitary bee *Centris pallida* during foraging and intermale mate competition. *Physiological Zoology*, *57*(2), 215–225.
24. May, M. (1995). Simultaneous control of head and thoracic temperature by the green darner dragonfly *Anax junius* (Odonata: Aeshnidae). *Journal of Experimental Biology*, *198*(11), 2373-2384.
25. Roberts, S.P., Harrison, J.F., & Hadley, N.F. (1998). Mechanisms of thermal balance in flying *Centris pallida* (Hymenoptera: Anthophoridae). *Journal of Experimental Biology*, *201*(15), 2321-2331.
26. Borrell, B.J. and Medeiros, M.J. (2004). Thermal stability and muscle efficiency in hovering orchid bees (Apidae: Euglossini). *Journal of Experimental Biology*, *207*(17), 2925-2933.
27. Dudley, R. and Ellington, C.P. (1990). Mechanics of forward flight in bumblebees: II. Quasi-steady lift and power requirements. *Journal of Experimental Biology*, *148*(1), 53-88.
28. Ellington, C.P. (1984a). The aerodynamics of hovering insect flight. III. Kinematics. *Philosophical Transactions of the Royal Society of London. B, Biological Sciences*, *305*(1122), 41-78.
29. Chai, P., Chen, J.S.C., and Dudley, R. (1997). Transient hovering performance of hummingbirds under conditions of maximal loading. *Journal of Experimental Biology*, *200*(5), 921-929.
30. Iriarte-Diaz, J., Riskin, D.K., Breuer, K.S., and Swartz, S.M. (2012). Kinematic plasticity during flight in fruit bats: individual variability in response to loading. *PLoS One*, *7*(5), e36665.
31. Combes, S.A., Gagliardi, S.F., Switzer, C.M., and Dillon, M.E. (2020). Kinematic flexibility allows bumblebees to increase energetic efficiency when carrying heavy loads. *Science Advances*, *6*(6), eaay3115.
32. Fry, S.N., Sayaman, R., and Dickinson, M.H. (2005). The aerodynamics of hovering flight in *Drosophila*. *Journal of Experimental Biology*, *208*(12), 2303-2318.
33. Bomphrey, R.J., Nakata, T., Phillips, N., and Walker, S.M. (2017). Smart wing rotation and trailing-edge vortices enable high frequency mosquito flight. *Nature*, *544*(7648), 92-95.
34. Altshuler, D.L., Dickson, W.B., Vance, J.T., Roberts, S.P., and Dickinson, M.H. (2005). Short-amplitude high-frequency wing strokes determine the aerodynamics of honeybee flight. *Proceedings of the National Academy of Sciences*, *102*(50), 18213-18218.
35. Vance, J.T., Altshuler, D.L., Dickson, W.B., Dickinson, M.H., and Roberts, S.P. (2014). Hovering flight in the honeybee *Apis mellifera*: kinematic mechanisms for varying aerodynamic forces. *Physiological and Biochemical Zoology*, *87*(6), 870-881.
36. Winston, M.L. (1991). *The biology of the honey bee*. Cambridge, MA: Harvard University Press.
37. Jørgensen, L.B., Malte, H., Ørsted, M., Klahn, N.A., and Overgaard, J. (2021). A unifying model to estimate thermal tolerance limits in ectotherms across static, dynamic and fluctuating exposures to thermal stress. *Scientific Reports*, *11*(1), 1-14.
38. Kovac, H., Käfer, H., Stabentheiner, A., and Costa, C. (2014). Metabolism and upper thermal limits of *Apis mellifera carnica* and *A. m. ligustica*. *Apidologie*, *45*, 664-677.

39. Burdine, J.D. and McCluney, K.E. (2019). Differential sensitivity of bees to urbanization-driven changes in body temperature and water content. *Scientific Reports*, *9*(1), 1-10.
40. Ellington, C.P. (1984b). The aerodynamics of hovering insect flight. VI. Lift and power requirements. *Philosophical Transactions of the Royal Society of London. B, Biological Sciences, 305*(1122), 145-181.
41. Lehmann, F.-O. and Dickinson, M.O. (1997). The changes in power requirements and muscle efficiency during elevated force production in the fruit fly *Drosophila melanogaster*. *Journal of Experimental Biology*, *200*(7), 1133–1143.
42. Coelho, J.R. (1991). The effect of thorax temperature on force production during tethered flight in honeybee (*Apis mellifera*) drones, workers, and queens. *Physiological Zoology*, *64*(3), 823-835.
43. Lighton, J.R. (2018). *Measuring Metabolic Rates: A Manual for Scientists*. Oxford University Press.
44. Beenakkers, A.M.T., Van der Horst, D.J., and Van Marrewwijk, W.J.A. (1984). Insect flight metabolism. *Insect Biochemistry* 14, 243–260.
45. Bertsch, A. (1984). Foraging in male bumblebees (*Bombus lucorum* L.): Maximizing energy or minimizing water load? *Oecologia* 62, 325–336.
46. Rothe, U. and Nachtigall, W. (1989). Flight of the honeybee. IV. Respiratory quotients and metabolic rates during sitting, walking and flying. *Journal of Comparative Physiology B,* 158, 739–749.
47. Heikkila, J., and Silvén, O. (1997). A four-step camera calibration procedure with implicit image correction. In *Proceedings of IEEE computer society conference on computer vision and pattern recognition* (1106-1112). IEEE.
48. Zhang, Z. (2000). A flexible new technique for camera calibration. *IEEE Transactions on pattern analysis and machine intelligence*, *22*(11), 1330-1334.
49. Hedrick, T.L. (2008). Software techniques for two-and three-dimensional kinematic measurements of biological and biomimetic systems. *Bioinspiration & Biomimetics*, *3*(3), 034001.
50. Burnett, N.P., Badger, M.A., and Combes, S.A. (2020). Wind and obstacle motion affect honeybee flight strategies in cluttered environments. *Journal of Experimental Biology*, *223*(14), jeb222471.
51. Ravi, S., Siesenop, T., Bertrand, O.J., Li, L., Doussot, C., Fisher, A., Warren, W.H., and Egelhaaf, M. (2022). Bumblebees display characteristics of active vision during robust obstacle avoidance flight. *Journal of Experimental Biology*, *225*(4), jeb243021.
52. Feuerbacher, E., Fewell, J. H., Roberts, S. P., Smith, E. F., & Harrison, J. F. (2003). Effects of load type (pollen or nectar) and load mass on hovering metabolic rate and mechanical power output in the honey bee *Apis mellifera*. *Journal of Experimental Biology*, *206*(11), 1855-1865.

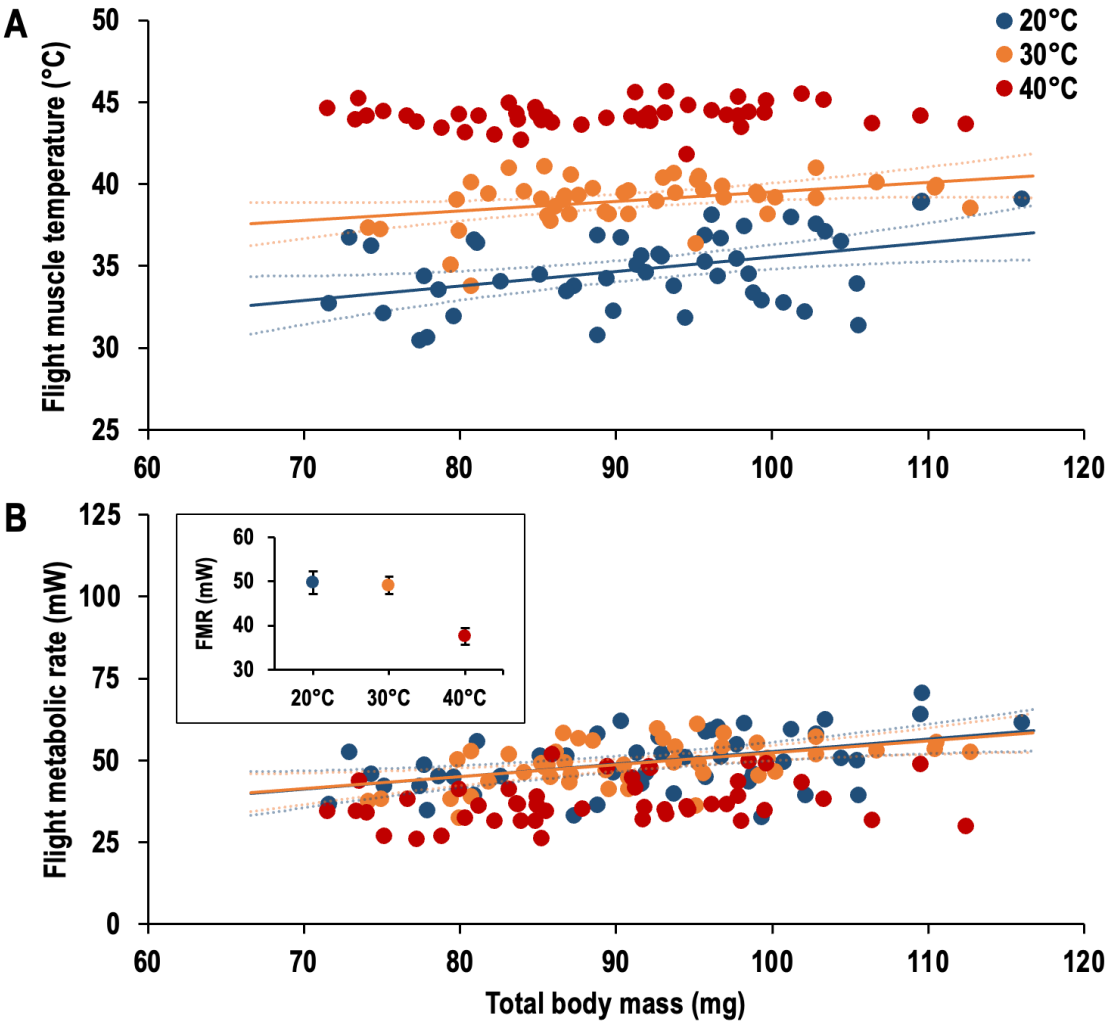

Figure 1. Air temperature and nectar-load effects on (**A**) flight muscle temperature and (**B**) metabolic rate. Total body mass is the mass of the unloaded bee (similar in all workers; ~ 70 mg) plus the nectar load it is carrying. Each point represents an individually measured bee. Regression lines and their corresponding 95% confidence limits denote statistically significant correlations between the independent variable and total body mass - the regression lines for flight metabolic rate at 20 and 30°C air temperature overlap. The points in the inset graph represent the mean ± 95% CL.

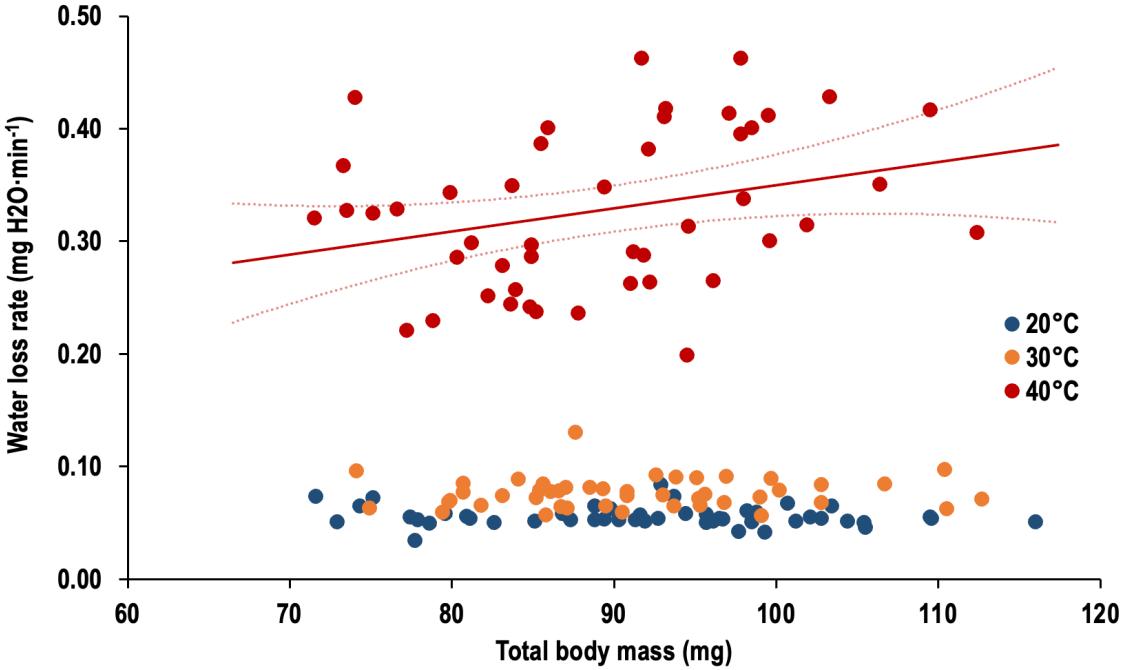

Figure 2. Water loss rates of honey bees increased with nectar load at 40°C, but not 20 or 30°C air temperature. Total body mass is the mass of the unloaded bee plus the nectar load it is carrying. Each point represents an individually measured bee. The regression line and its corresponding 95% confidence limits denote a statistically significant effect of total body mass on water loss rate.

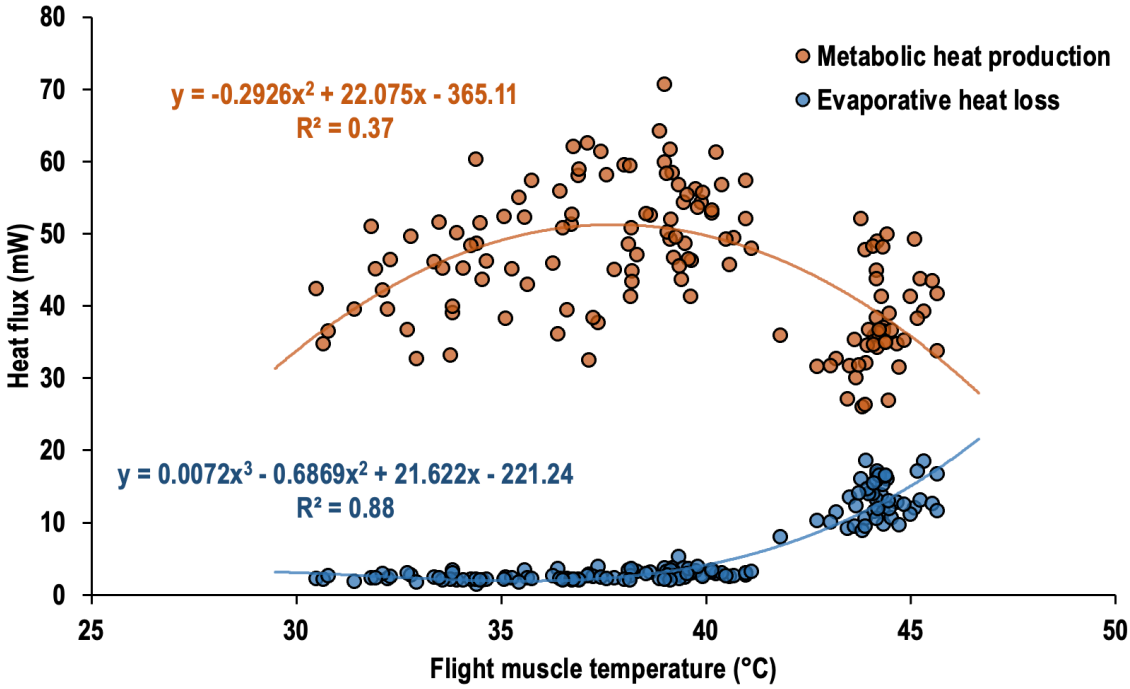

696

697 **Figure 3.** The interactive effects of flight muscle temperature on metabolic heat production and

698 evaporative heat loss of loaded and unloaded flying honey bees, with data pooled over all

699 external air temperatures. Each point represents an individually measured bee.

700

701

702

703

704

705

706

707

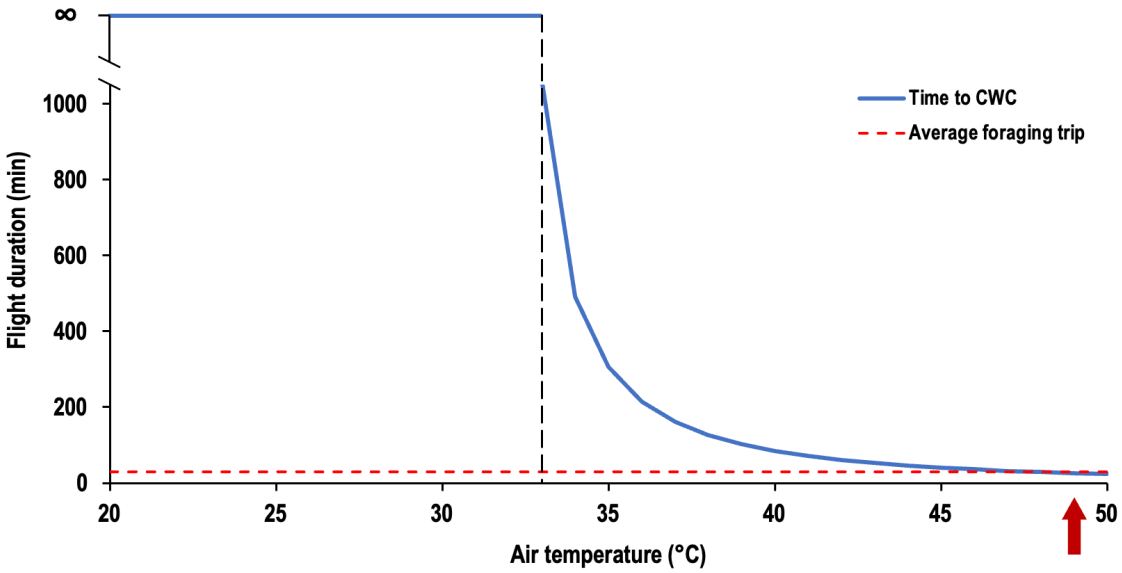

708

709 **Figure 4.** The length of time an unloaded forager (average: 70 mg) can fly at a given air
710 temperature before reaching critical water content (CWC) when flying in dry air (blue line). The
711 red dotted line represents the average foraging trip for a honey bee (30 min; 36). The red arrow
712 denotes the upper critical thermal limit for honey bees at rest (approximately 49°C; 38,39).

713

714

715

716

717

718

719

720

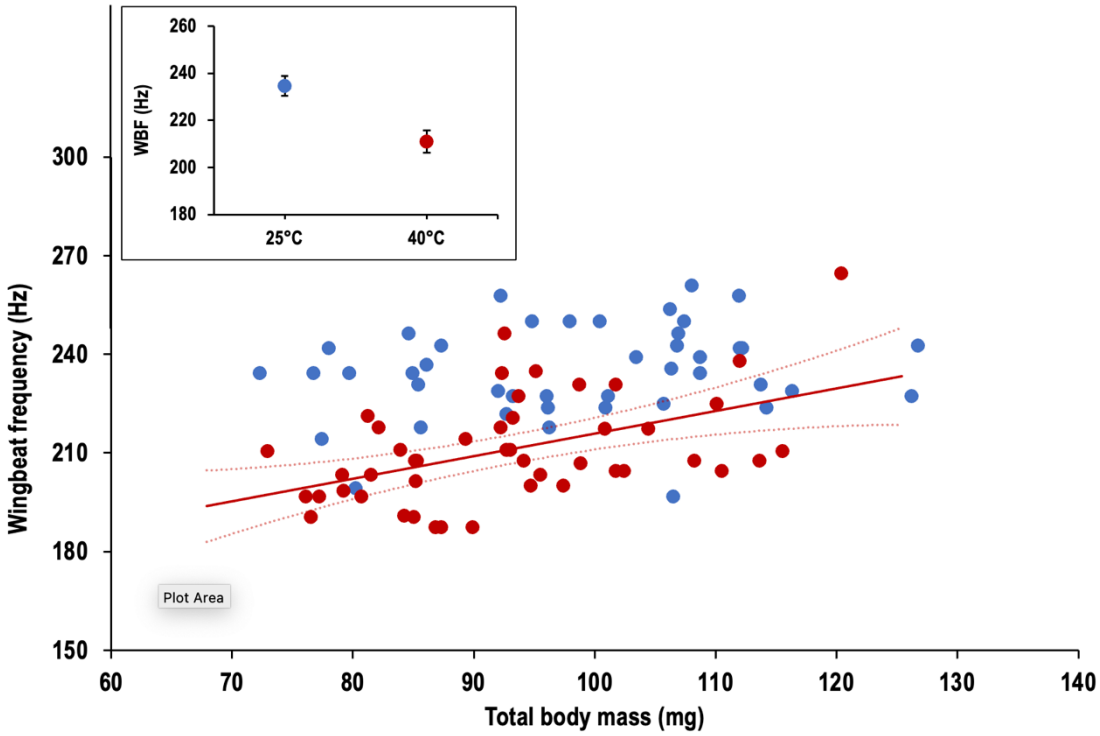

721

722 **Figure 5.** Air temperature affected bees' wingbeat frequencies and their kinematic responses to
723 loading. Honey bees had lower wingbeat frequencies at 40°C air temperature than at 25°C. Total
724 body mass is the mass of the bee plus the nectar load it is carrying. Each point represents an
725 individually measured bee. The regression line and its corresponding 95% confidence limits
726 denote statistically significant correlations between wingbeat frequency and total body mass.

727

728

729

730

731

732

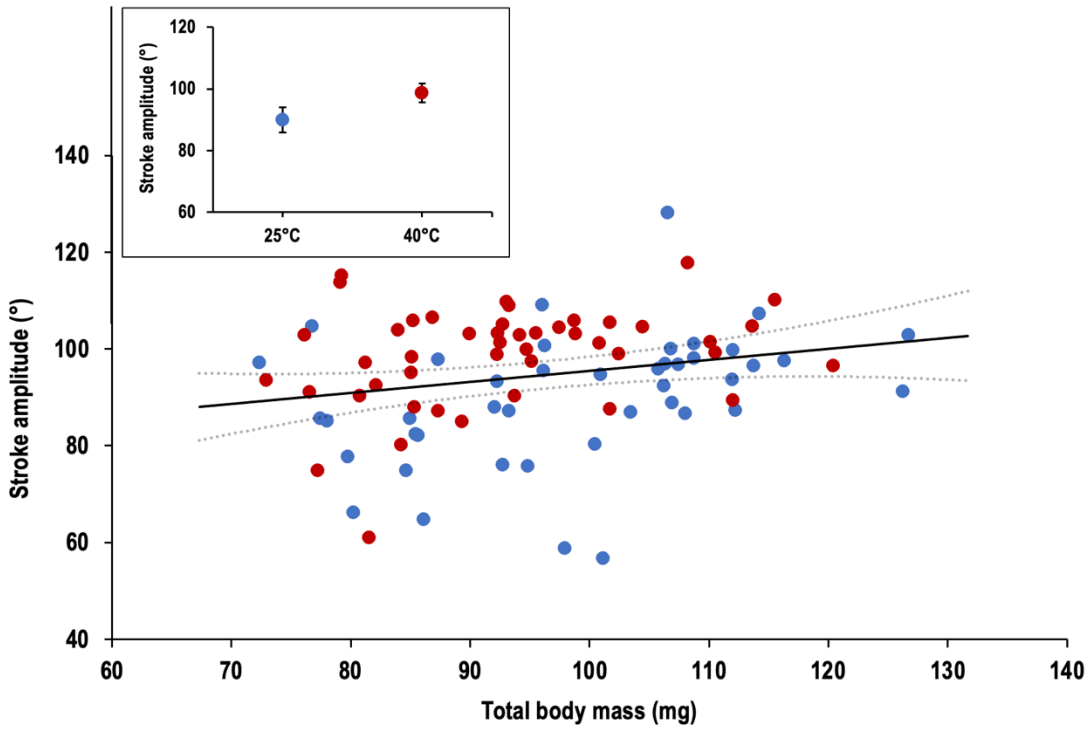

733

734 **Figure 6.** Honey bees had larger stroke amplitudes at 40°C air temperature than at 25°C (inset),
735 and bees at both temperatures increased stroke amplitude with increasing total body mass. Total
736 body mass is the mass of the bee plus the nectar load it is carrying. Symbols in the inset graph
737 represent the mean ± 95% CL. For the generalized linear regression plot, each point represents
738 an individually measured bee. The regression line and its corresponding 95% confidence limits
739 denote statistically significant correlations between stroke amplitude and total body mass.

740

741

742

743

744

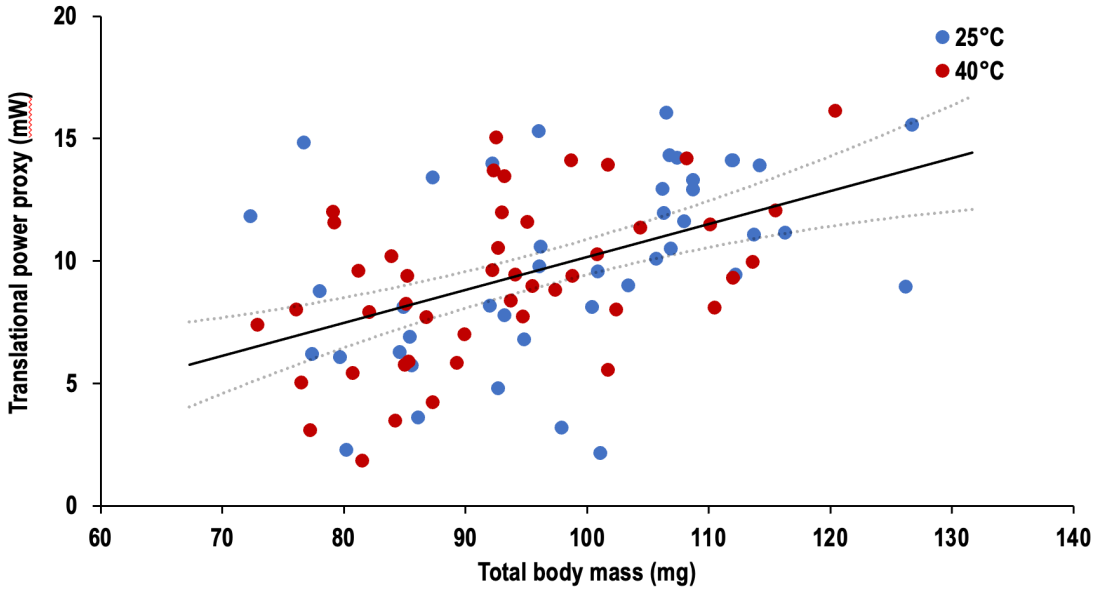

745

746 **Figure. 7.** Honey bees flying at 25 and 40°C air temperature display a similar increase in
747 translational force production with increasing total body mass (main figure). The dashed line
748 delineates the total force (mN) required to support the weight of the bee plus its nectar load. Each
749 point represents an individually measured bee. The fitted line in the main graph and its
750 corresponding 95% confidence limits denote statistical significance for the independent effect of
751 total body mass on translational force production. The inset graph shows the proportion of total
752 force accounted for by our estimated force production during wing translation (F_{tr}/F). This
753 proportion was the same in nectar-loaded bees flying at 25 and 40°C air temperature (GLM: n =
754 89, df = 1, χ^2 = 8.2, p = 0.61). The dotted line fitted to the data in the inset graph is there for
755 visualization and does not denote statistical significance.

756

757

758

759

760 **Table S1.** The linear fit, coefficient of determination, and the p-value corresponding to its
761 corresponding figure within the manuscript.
762

Figure	Air temperature (°C)	Linear fit	R^2	*p*
1A	20	y = 0.0881x + 26.734	0.17	< 0.001***
1A	30	y = 0.0587x + 33.667	0.14	< 0.01**
1B	20	y = 0.3846x + 14.266	0.21	< 0.001***
1B	30	y = 0.3644x + 15.831	0.24	< 0.01**
2	40	y = 0.0021x + 0.1441	0.09	0.046*
5	40	y = 0.6875x + 147.13	0.24	< 0.01**
6	pooled	y = 0.2279x + 72.711	0.05	< 0.01**
7	pooled	y = 0.0065x + 0.0318	0.23	< 0.001***
S2	pooled	y = 0.1342x - 3.2595	0.23	< 0.001***
S3	pooled	y = 0.2696x + 2.2315	0.22	< 0.001***

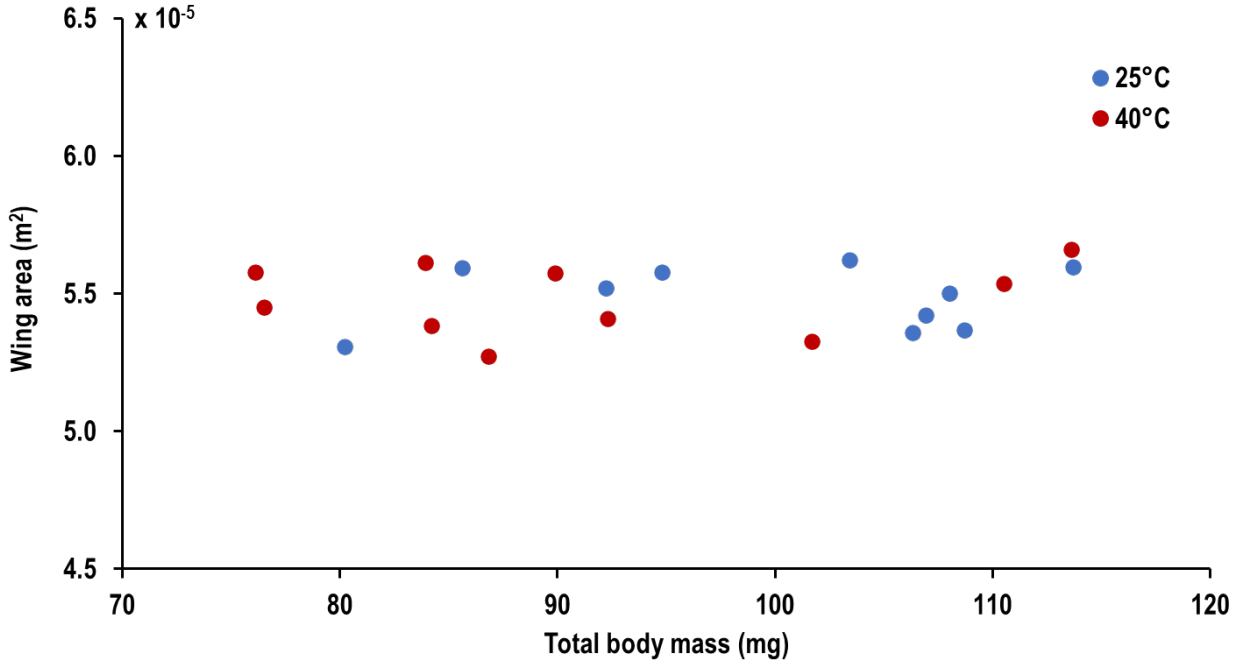

Figure S1. Nectar forager body size (wing area) was independent of total body mass (i.e., the bee plus the mass of the nectar load they carried; LM: $n = 20$, $F_{1,18} = 0.40$, $p = 0.53$) for bees flown at 25 ($n = 10$) and 40°C ($n = 10$) air temperature. Each point represents an individually measured bee.

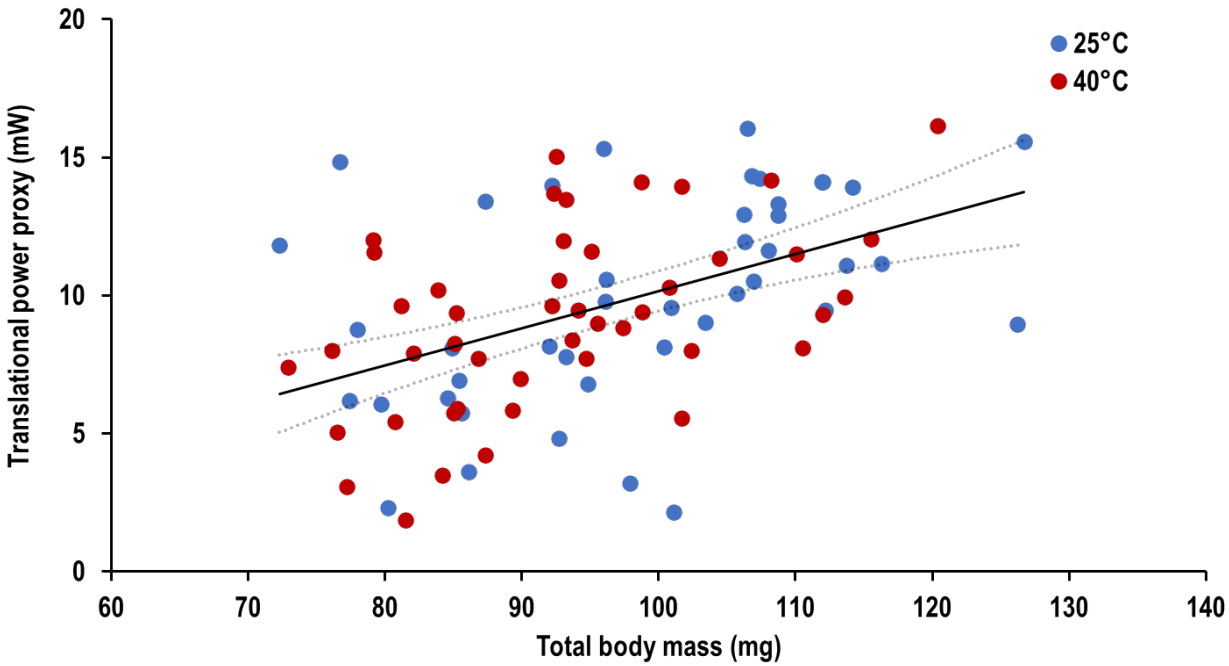

Figure S2. Honey bees flying at 25 and 40°C air temperature increased translational power production with increasing total body mass. Each point represents an individually measured bee. The fitted line and its corresponding 95% confidence limits denote statistical significance for the independent effect of total body mass on the translational power production.

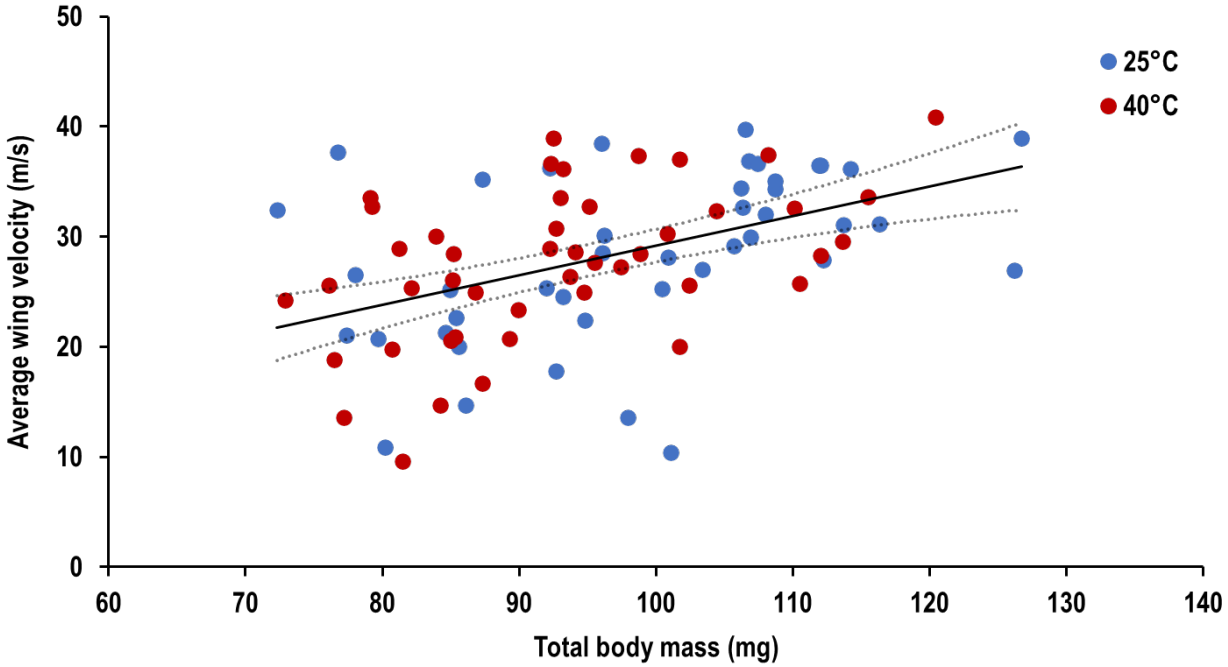

Figure S3. Honey bees flying at 25 and 40°C air temperature increased average wing velocity with increasing total body mass. Each point represents an individually measured bee. The fitted line and its corresponding 95% confidence limits denote statistical significance for the independent effect of total body mass on the average wing velocity.